Microstructural, Mineralogical and Geochemical Characterization of Au-Ag-Pb-Zn Mineralization from Moulay Bou Azza, Morocco

E. Mahjoubi[1#], M. AIT ADDI[2], A. OULGOR[2], H. KHEBBI[3], H. OUAZZANI[1], A. OUDY[1], I. AMRI[2], A. ZERDANE[3] A. CHAIB[3]

1: Moulay Ismail University, Faculty of Sciences Meknes, B.P. 11201 Zitoune, Meknes, Morocco; **#:** mahjoubi_elmahjoub@yahoo.fr
2: Abdelmalek Essaadi University, Faculty of Sciences Tetouan; **3**: National Office of Hydrocarbons and Mines - (ONHYM) Rabat

THE GEOLOGICAL SOCIETY OF AMERICA® CONNECTS 2022 9–12 October Denver, Colorado, USA & Online Everywhere

1 Introduction and geological setting

- The Moulay Bou Azza (MBA) district is located in the Moroccan Central Hercynian massif on the vicinity of Smaala-Oulmes ductile shear zone (Fig.1).
- Terranes of studied areas consist of Ordovician-Namurian formations intruded by dykes and MBA granite (Fig.2).
- Vein mineralization is hosted in Silurian black-shales within Bled Jemaa **BJ** and in Namurian pelites-sandstones in Ighir Ou Roumi **IR**.

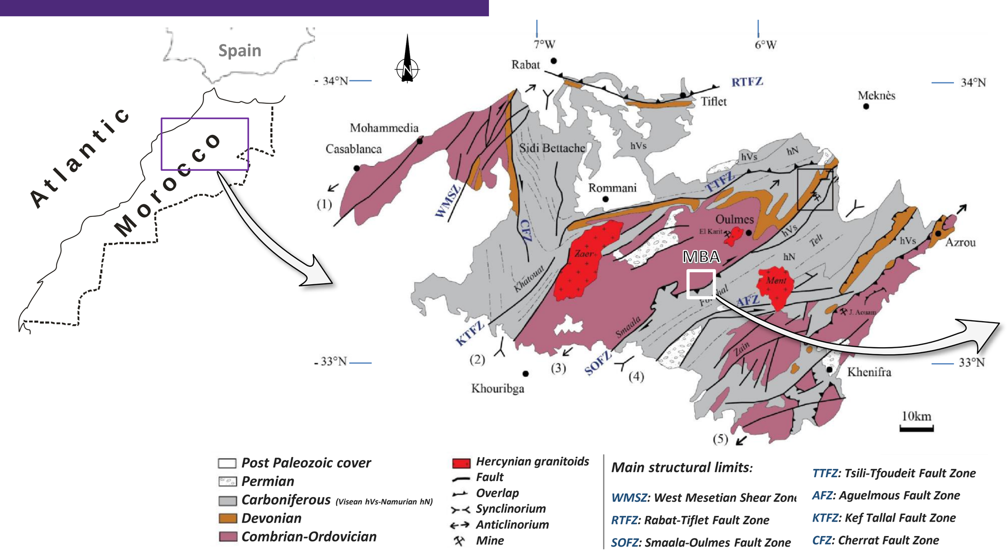

Fig.1. Structural units of Central Morocco (Michard, 1976)

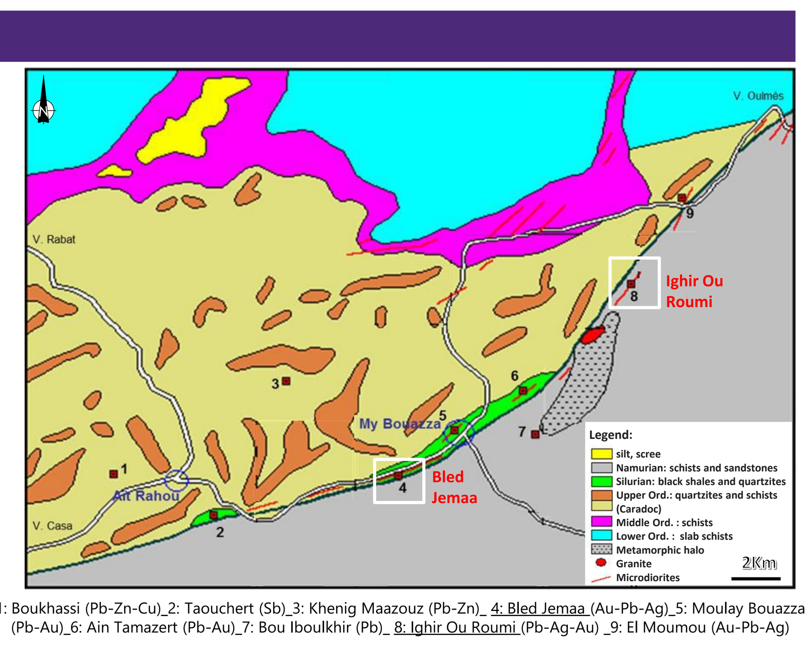

Fig.2. Geological sketch of MBA district and situation of the mineralized sites (Fettouhi, 2011). Inset 4 and 8 : BJ and IR areas.

2 Goal and methods

- The aim of this study is to understand the nature and paragenetic evolution of mineralization and expression nature of Au and Ag mineralization.
- We carried out a microstructural analysis combined with textural study of drill core and hand specimens from vein mineralization.
- Geochemical analysis focus on minerals bearing Au and Ag using an optical microscope and scanning electron microscopy (SEM).

3 Vein geometry

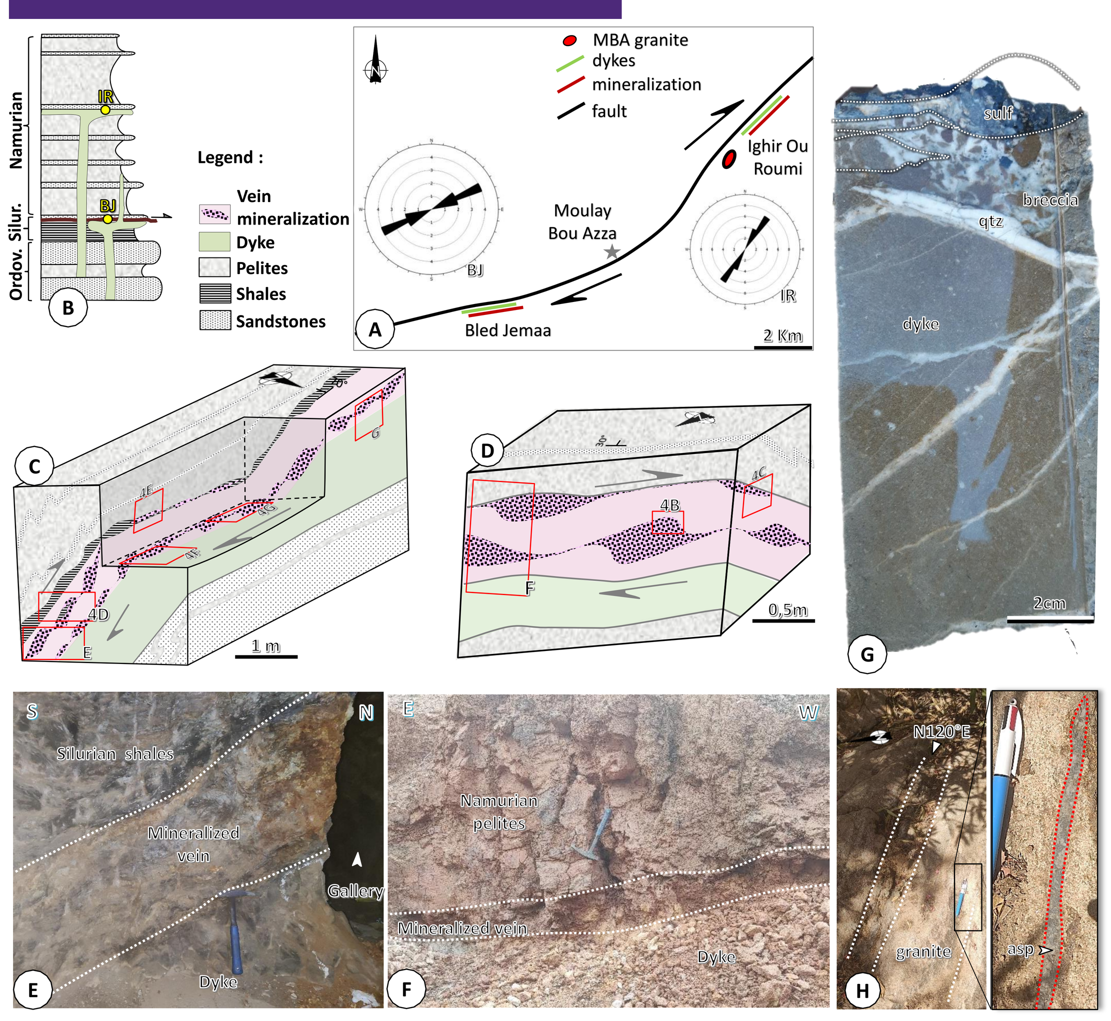

Field observations display two main fault families in both sites (Fig.3A):

- F1 dextral N30°E more present in IR (3A,D,F) and crosscut MBA granite (4A),
- F2 dextral N70°E more expressed in BJ (3A,C,E,G),
- Sinistral N120°E faults are minors, it crosscut MBA granite (3H).

The first and the second family, subparallel to the MBA shear zone in both areas (3A), are the main mineralization-bearing structures.

Fig.3. A. rose diagram for main faults orientations in BJ and IR (see Fig.2), B. stratigraphic log , C. and D. 3D structural model of BJ and IR with vein mineralization and dyke, E. and F. vein mineralization intersecting dykes and Silurian shales (in BJ) and Namurian pelites (in IR), G. drill core sample showing dyke sheared, brecciated and mineralized, H. granite intersected by N120°E faults and arsenopyrite vein.

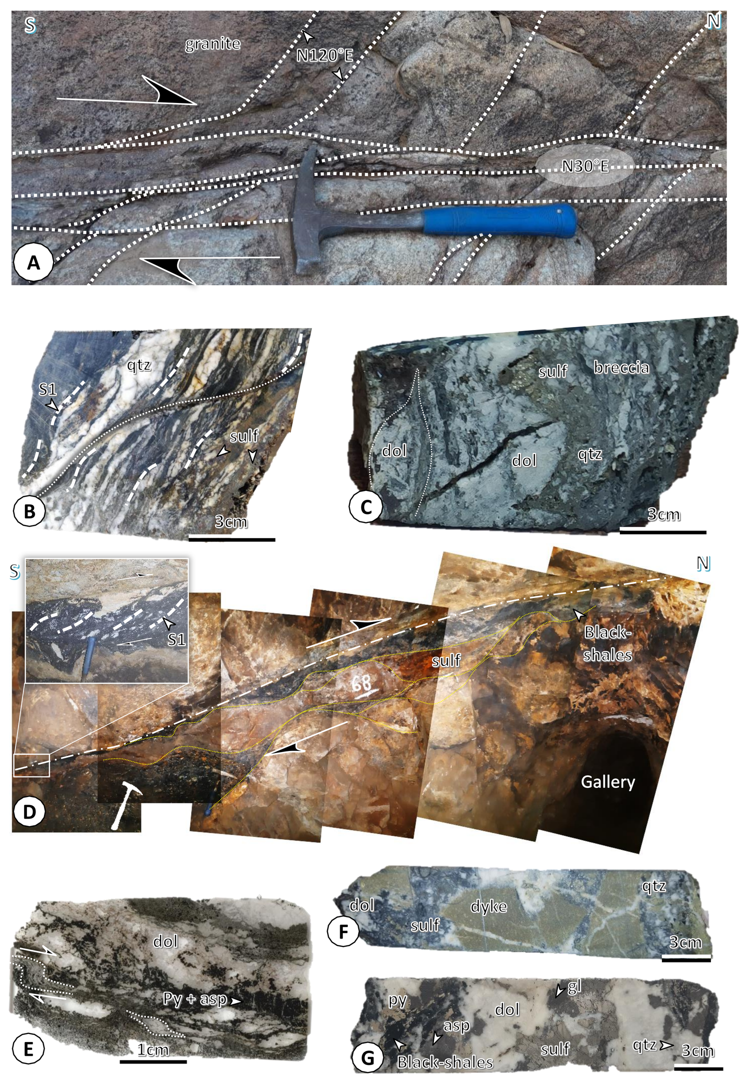

Veins geometry and their internal texture study exhibit :

i) sigmoidal lenses of quartz, dolomite and sulfides infilling (4B,D,E) with a thickness of 10 to 60cm,

ii) an evolution of deformation from ductile-brittle shear towards intense brecciation (4C,E,F),

iii) mineralization intersecting MBA granite (3H)and dykes (4F),

iv) Silurian black-shales with massive mineralization and breccia well marked in BJ (4D,F,G).

Fig.4. A, B and C in IR site. A. N30°E dextral fault intersecting granite, B. shear zone and associated mineralization, C. sigmoid lenses and breccia with sulfides cement. D, E, F and G in BJ site. D. wall of gallery showing N70°E vein mineralization and Silurian black-shales in shear zone, E. thin section displaying dol, py and asp deformed, F. and G. breccia and massive texture respectively in drill core sample.

4 Mineralogy

Five main paragenetic stages, their textures and related tectonic-magmatic-hydrothermal processes are illustrated in figures 5 and 6 :

i) asp1-qtz1 ;

ii) qtz2-dol -py1 ;

iii) qtz3-dol and massive sulfides with sph-gl1-py2- asp 2 and cp ;

iv) dol-el-gl2-cp infilling the late micro-fractures of py2 and asp2, and ;

v) qtz4-dol-el-gl3-sph-cp and fbg within the breccia.

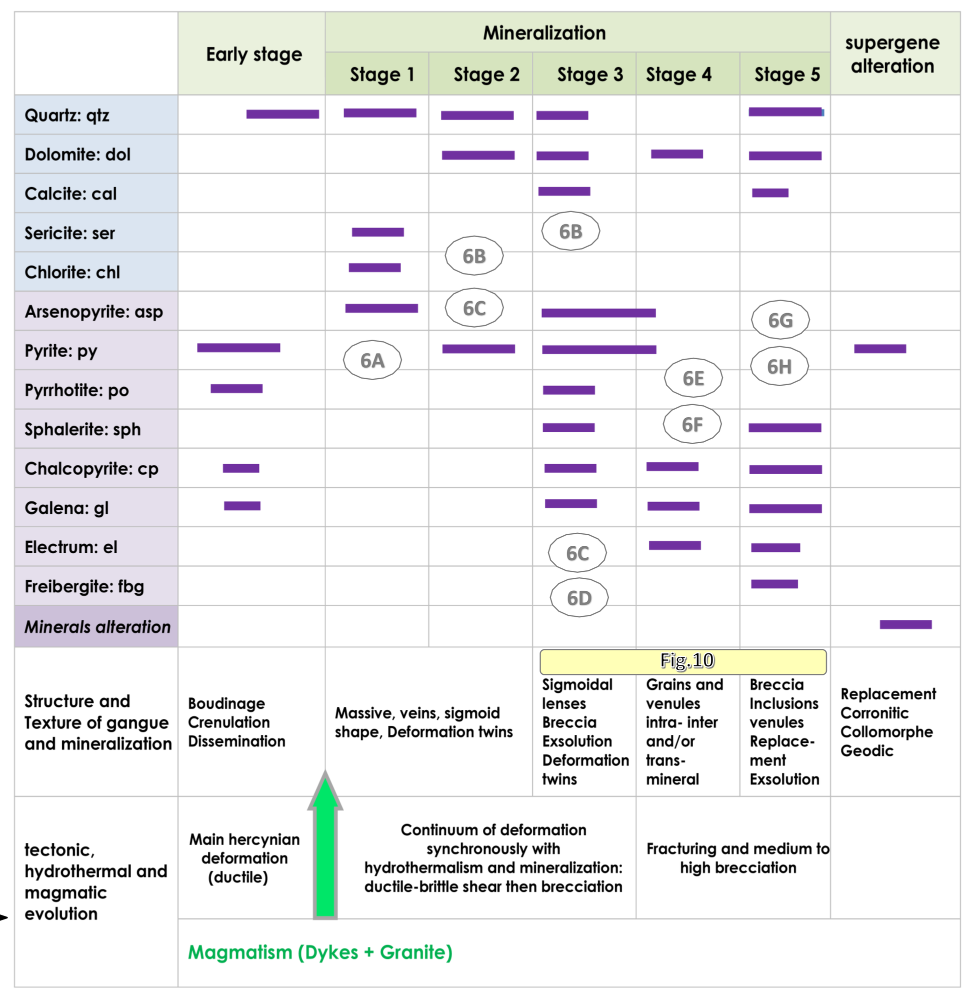

Fig.5. Paragenetic stages and associated textures (Fig.6), tectonic, magmatic and hydrothermal evolution in BJ and IR. Concentration process of electrum (stages 3 to 5) is sketched in the discussion.

5 Microtexture and geochemistry

Microtexture of minerals in mineralized vein (Figs.6,7) supported by SEM image (Fig.8) and punctual SEM analysis (Fig.9) lets us to confirm the paragenetic evolution (Fig.5) and nature of minerals bearing Au and Ag. Microtextural features (Fig.7) and geochemical data of sulfides suggest that gold displays:

i) lattice-bound form within py2 and asp2,

ii) micro inclusions form or micro-veinlets (intra- inter- and trans-mineral) in brecciated py2 and asp2, and

iii) free grains form of electrum up to 30µm within qtz4 and dol of breccia.

Electrum is composed of Au (45-72%) and Ag (52-25%).

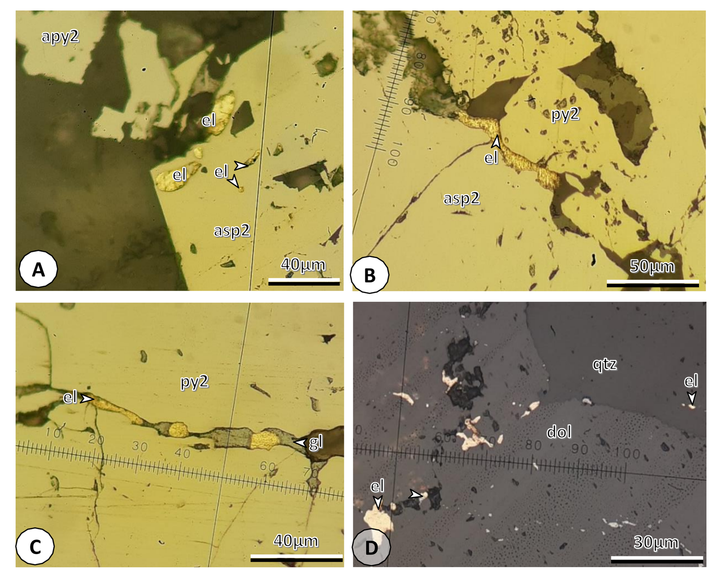

Fig.7. microphotographs on reflected light showing microtexture of electrum: A. intra mineral in py and asp, B. inter-minerals py -asp, C. trans-mineral via py, D. within breccia in qtz and dol of stage 5.

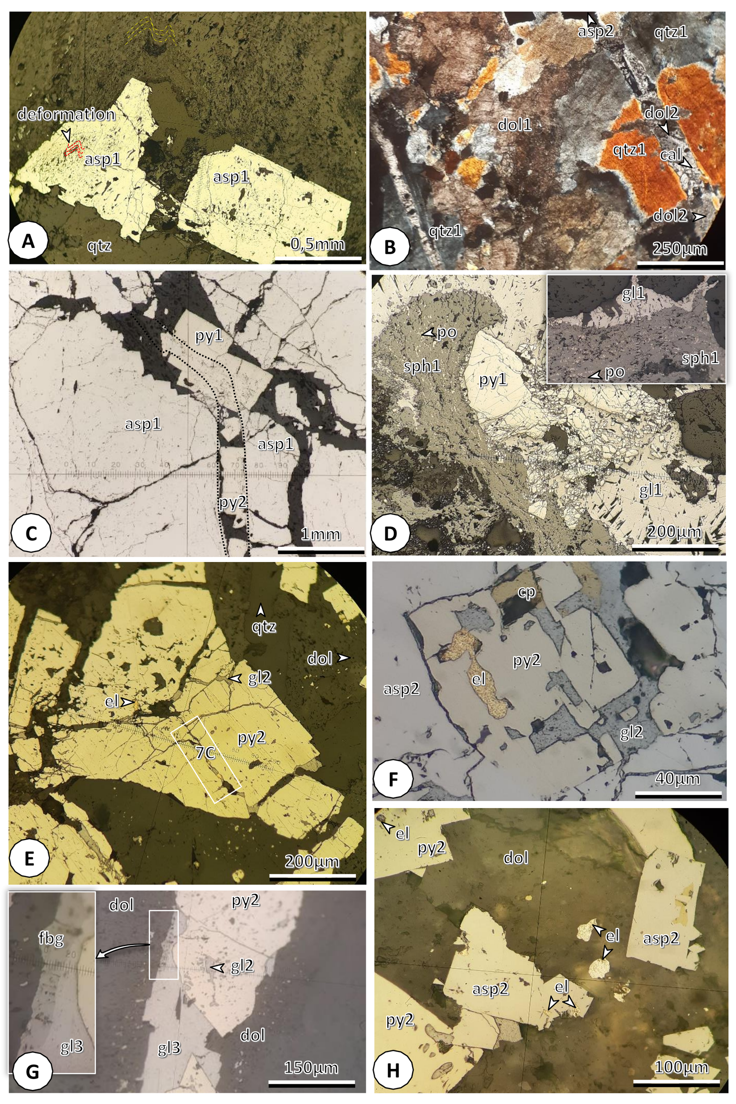

Fig.6. microphotographs showing microtexture of minerals. A. deformed asp, B. relictual grains of qtz1 within dol1, all crosscuted by asp2 and dol2, C. py2 intersecting asp1, D. sph-py-gl of stage 3 with deformation traces indicated by po, E. py2 intersected by veinlet of stage 4, F. el, gl and cp within py2, G. fbg and gl3 of stage 5, H. el inclusion in py2, asp2 and breccia.

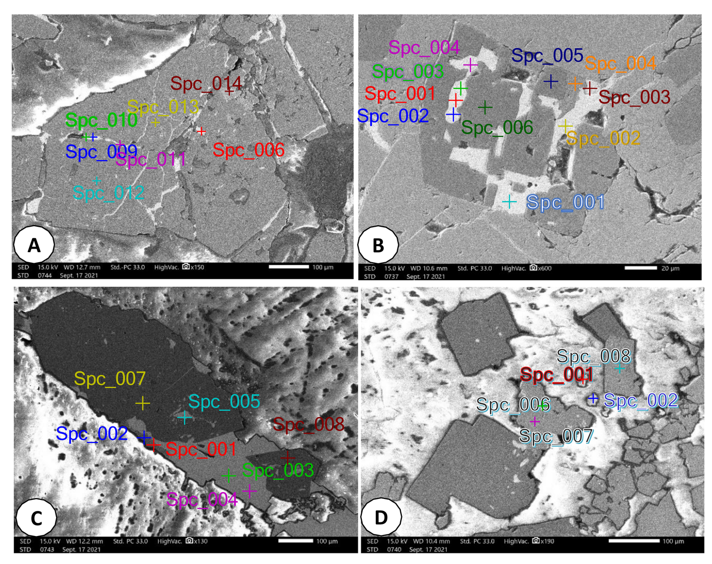

Fig.8. SEM images of minerals with analyzed points location. A, B, C and D images corresponds to E, F, G and H of Fig.6 respectively.

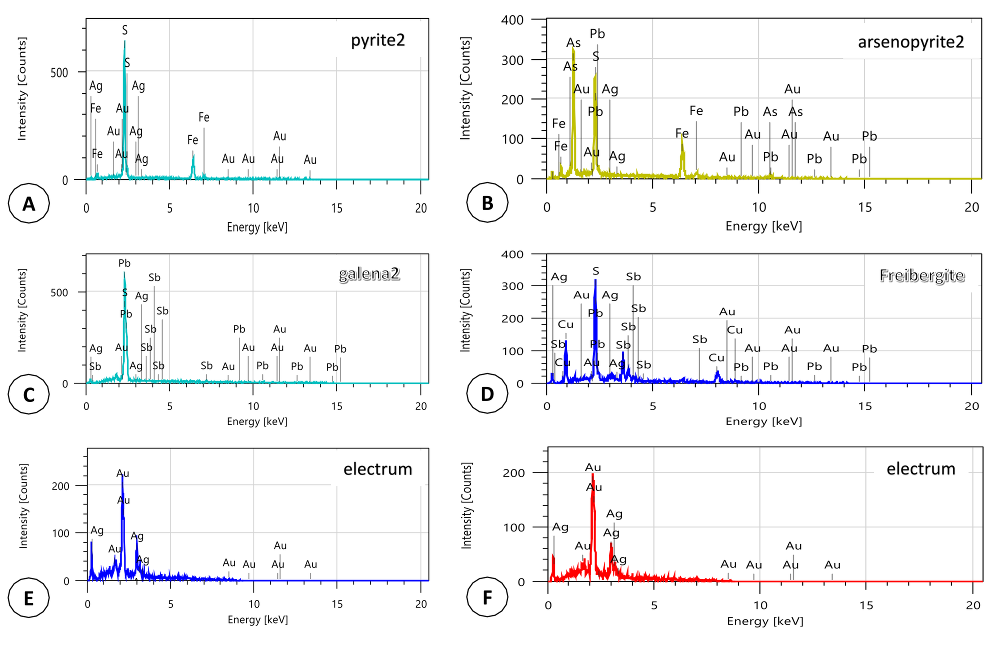

Fig.9. SEM analysis spectra of : A. pyrite, B. arsenopyrite, C. galena, D. freibergite, E and F. electrum from samples of BJ and IR sites.

6 Discussion and conclusion

The structural context of Bled Jemaa and Ighir Ou Roumi mineralization evolves from ductile-brittle shear (stage 1 to 3) to the brecciation (stages 4-5)

Formation mechanism that could explain diverse forms of gold during such evolution integrates (Fig.10):

- remobilization of "invisible" gold from py2 and asp2 (stage 3),
- its concentration as micro-inclusions and veinlet as el in py and asp (stage 4) and,
- reconcentration of electrum as free grains within breccia (stage 5).

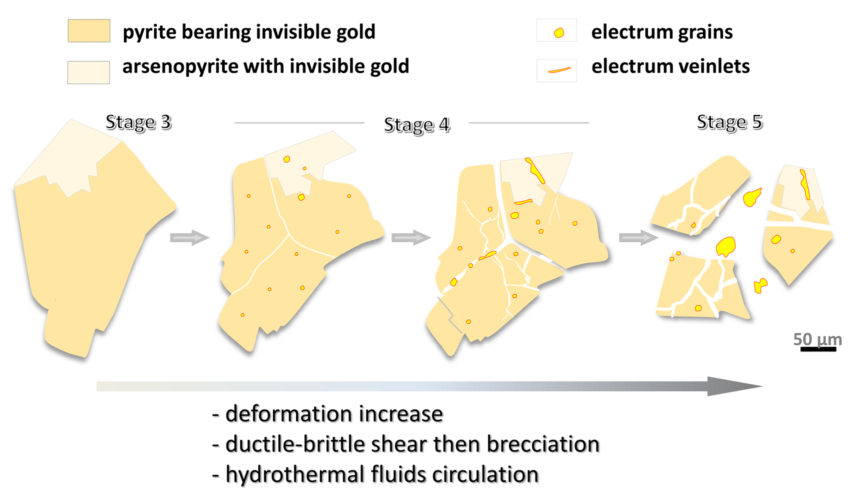

Fig.10. sketch displaying formation of electrum from invisible gold in py2 and asp2 in response to evolving deformation and hydrothermal circulations through shear zones and fracture system in BJ and IR .

This evolution could be resulted from a continuum of increasing deformation and hydrothermal circulations via sheared and fractured Silurian shales, rich in organic matter. Indeed, it is well known that majority of the “invisible” gold migrates first towards the fractures and voids within the same sulfides, then to the grain boundaries and ultimately migrates out of the host sulfides [1]. Post-depositional remobilization and concentration depends on hydrothermal fluid [2], deformation [3,4], metamorphism [5] and fluid-rock interaction especially shales rich on organic matter [4,6]. However further detailed studies are required.

To conclude, this study highlights that mineralization is emplaced under a marked structurally control with notable reactivation of pre-existing shear zones [7]. It also demonstrates how such control of ore deposition could be recorded from structural analysis, vein geometry, internal texture, and mineralogy.

Acknowledgement

Special thanks to professor BADRA Lakhlifi for correction of this work. Thanks also to Ilyas CHABRI from the Center for Innovation and Technology Transfer of Moulay Ismail University, Meknes (CITT-UMI) for minerals analysis and SEM images.

References :

*[1] **Cook, N. J. et al. (2013)** Arsenopyrite-pyrite association in an orogenic gold ore: Tracing mineralization history from textures and trace elements. Economic Geology, 108(6), 1273-1283. [2] **Sahoo, P. R., and Venkatesh, A. S. (2015)** Constraints of mineralogical characterization of gold ore: Implication for genesis, controls and evolution of gold from Kundarkocha gold deposit, eastern India. Journal of Asian Earth Sciences, 97, 136-149. [3] **Mumin, A. H. et al. (1994)** Gold mineralization in As-rich mesothermal gold ores of the Bogosu-Prestea mining district of the Ashanti gold belt, Ghana: Remobilization of “invisible” gold. Mineralium Deposita, 29(6), 445-460. [4] **Mikulski, S. Z. (2007)** The late Variscan gold mineralization in the Kaczawa Mountains, Western Sudetes. Polish Geological Institute Special Papers, 22, 21-162. [5] **Murphy, P. J., and Roberts, S. (1997)** Evolution of a metamorphic fluid and its role in lode gold mineralisation in the Central Iberian Zone. Mineralium Deposita, 32(5), 459-474. [6] **Majumdar, S. et al. (2020)** Characterization of organic matter and its implications for pyrite hosted refractory gold mineralization along the South Purulia Shear Zone, eastern India. Ore Geology Reviews, 124, 103584. [7] **Chauvet, A. (2019)** Structural control of ore deposits: The role of pre-existing structures on the formation of mineralised vein systems. Minerals, 9(1), 56.*